ChemComm

Supporting Information

Sb nanoparticles embedded uniformly on the surface of porous carbon fibers for high-efficiency sodium storage

Yafei Zhao, Kai Xue, Xinyu Liu, Zhiyuan Gao, Junhao Zhang, Yuanjun Liu, Xiangjun Zheng, ZhongYao Duan, Qianqian Fan, Xingmei Guo**

School of Environmental and Chemical Engineering, Jiangsu University of Science and Technology, Zhenjiang 212003, China

Corresponding author: jhzhang6@just.edu.cn (J. Zhang)

guoxm@just.edu.cn (X. Guo)

Experimental section

Synthesis of Sb NPs-SCFs precursor

0.3 g of polyacrylonitrile (PAN) and 0.2 g of polymethyl methacrylate (PMMA) were dissolved in 5 mL of N, N-dimethylformamide and stirred at 60 °C to form a transparent solution. Subsequently, 0.8 g of antimony trichloride ($SbCl_3$) was added and stirred for 12 h to achieve a uniformly dispersed electrospinning solution. The transparent precursor solution was then loaded into a plastic syringe for electrospinning. The solution flow rate was set to 0.4 mL h^{-1}, and the fibers were collected on aluminum foil, maintaining a needle-to-fiber collector distance of 15 cm. A voltage of 15 kV was applied between the electrospinning needle and the aluminum foil to initiate the electrospinning process. Following electrospinning, the obtained Sb NPs-SCFs precursor were dried in a vacuum drying box at 60 °C for 12 h.

Synthesis of Sb NPs-SCFs composites

The obtained Sb NPs-SCFs precursor membrane underwent an initial stabilization process at 250 °C for 3 h, with a heating rate of 5 °C min^{-1} under air atmosphere. Subsequently, the temperature was raised to 600 °C for carbonization over 2 h with a heating rate of 5 °C min^{-1} in Ar atmosphere, obtaining Sb NPs-SCFs composite.

Material characterization

The phase and structure of the samples were investigated using X-ray diffractometer (XRD, SmartLab 9 KW, Cu target, U=40 kV, I=40 mA, measurement angle between 5° and 85°, 10 °min^{-1}). The morphology were examined through

scanning electron microscopy (SEM, XL30). For an in-depth analysis of the internal structure, high-resolution transmission electron microscopy (HRTEM, JEM2100F) was employed. Graphitization and defect degree were assessed using laser confocal Raman spectroscopy (Raman, Edinburgh RM5, λ=514 nm). X-ray photoelectron spectroscopy (XPS, Thermo Scientific Nexsa) was utilized to explore the surface chemical composition of the samples. The contents of Sb and C were quantified via thermogravimetric analysis (TGA).

Electrochemical measurements

The electrochemical performances of the anode materials were assessed by assembling CR2032 button cells. Initially, the anode material was prepared by combining Sb NPs-SCFs composites, carbon black (Super P) and carboxymethyl cellulose (CMC) in a mass ratio of 7:1.5:1.5. The weighed samples underwent a 30-minute grinding process in an agate mortar before being transferred to a stirring bottle. Subsequently, the mixture was stirred with an appropriate amount of deionized water for 12 h, forming a uniform electrode paste. The well-stirred slurry was then coated onto copper foil using a square preparation device. After pre-drying the anode material at 25 °C for 30 minutes, it was further dried in a vacuum drying box at 70 °C for 12 h, which was punched into round plates with a diameter of 12 mm, and the active material load per piece was controlled with about 0.8-1.2 mg. For assembly, sodium sheet and fiberglass filter paper (Whatman GF/F) were served as the counter electrode and diaphragm, respectively. The electrolyte was 1 mol L^{-1} $NaPF_6$ in polycarbonate (PC, 100 vol%). The battery assembly was taken place in a glove box

filled with Ar, ensuring a controlled environment with concentrations of water and oxygen lower than 0.1 ppm.

Galvanostatic charge/discharge tests and galvanostatic intermittent titration technique (GITT) measurements were conducted using the LAND electricity test system (CT2001A). Cyclic voltammetry (CV) and electrochemical impedance spectroscopy (EIS) were performed employing an electrochemical workstation (CHI 760E). The CV scans were conducted at a rate of 0.1 mV s^{-1}, covering the voltage range from 0.01 V to 3 V. Additionally, electrochemical impedance spectroscopy (EIS) measurements were carried out over a frequency range of 0.1-100 kHz. For the GITT measurement, the cell was discharged/charged with a constant current flux for 10 min followed by an open-circuit stand for 30 min.

Supplementary Figures

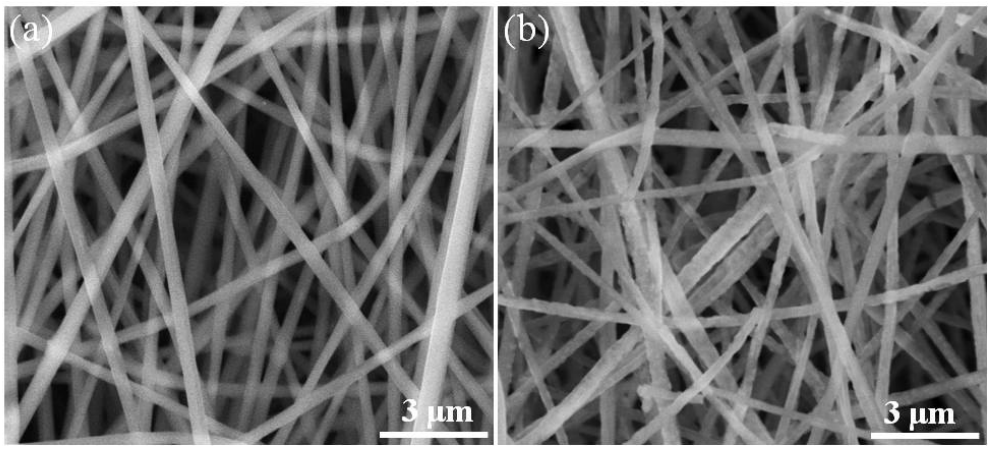

Fig. S1. SEM images: (a) PAN/PMMA/$SbCl_3$ film; (b) Pre-oxidized precursor film.

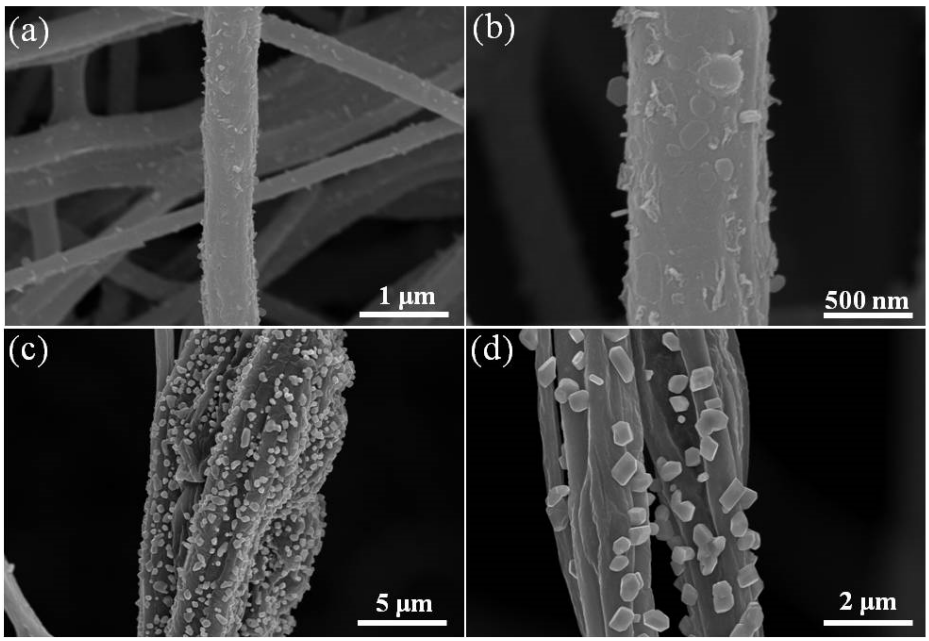

Fig. S2. SEM images: (a, b) Sb NSs-SCFs composite; (c-d) Sb MPs/SCFs composite

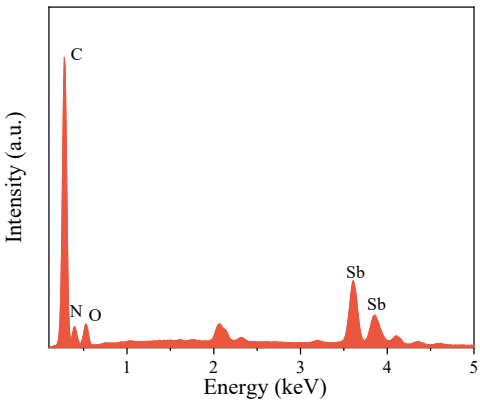

Fig. S3. EDS pattern of Sb NPs-SCFs composite

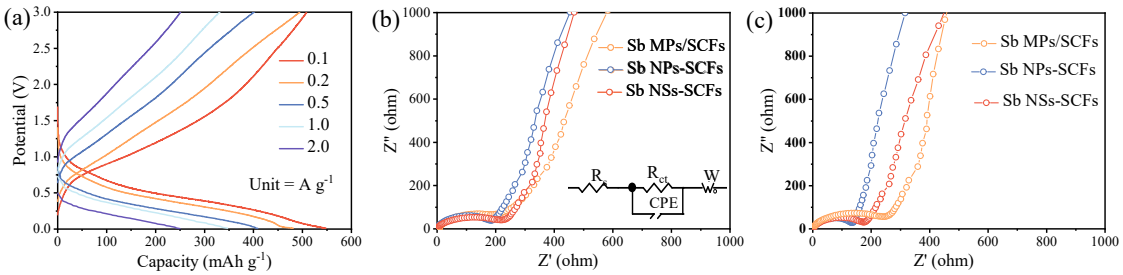

Fig. S4. (a) Charge-discharge curves of Sb NPs-SCFs anode at various current densities; (b, c) EIS of Sb NSs-SCFs, Sb NPs-SCFs and Sb MPs/SCFs anodes before cycling and after 100 cycles

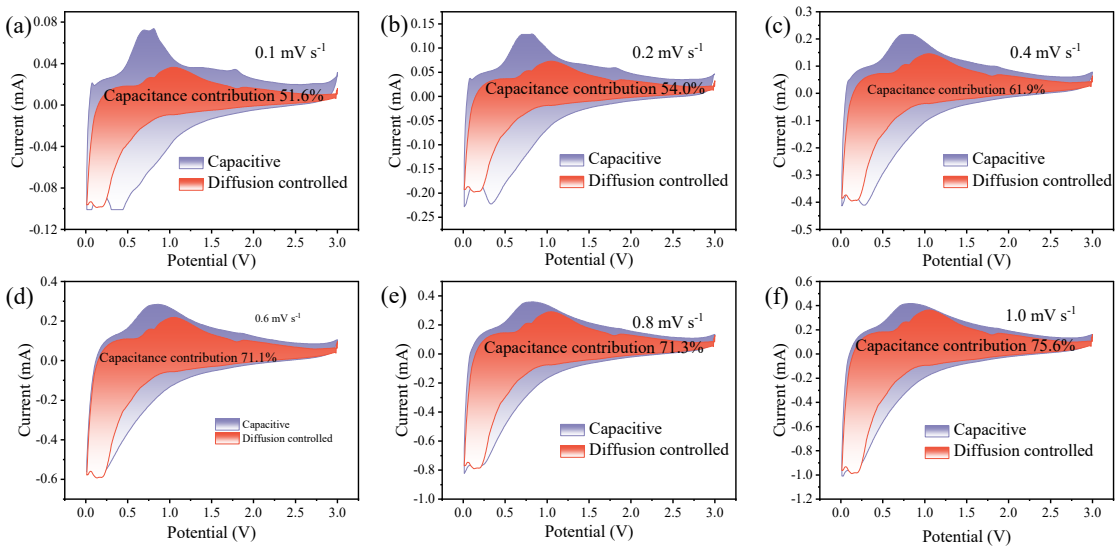

Fig. S5. Capacitive contribution to the total current contribution for Sb NPs-SCFs anode: (a) 0.1 mV·s^{-1}; (b) 0.2 mV·s^{-1}; (c) 0.4 mV·s^{-1}; (d) 0.6 mV·s^{-1}; (e) 0.8 mV·s^{-1}; (d) 1.0 mV·s^{-1}

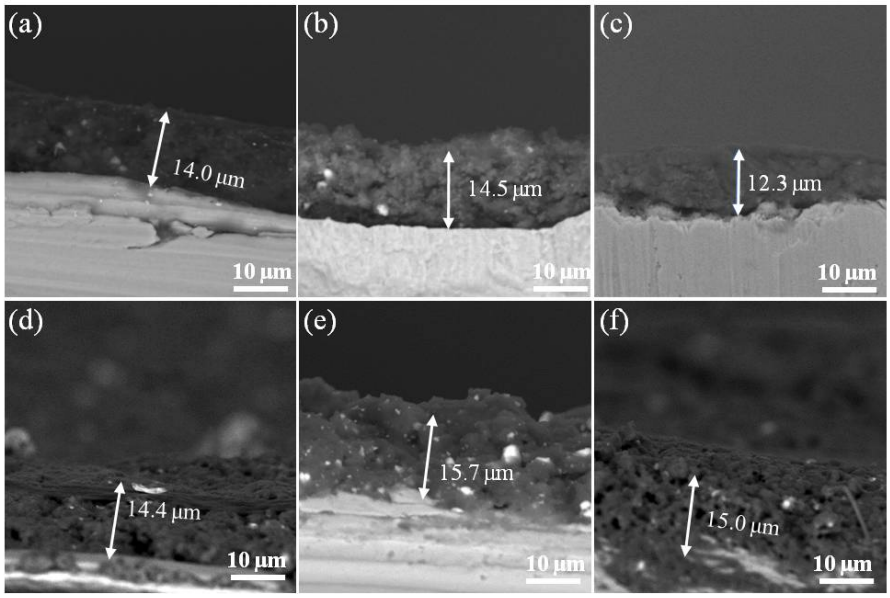

Fig. S6. (a-c) Electrode thickness of Sb NSs-SCFs, Sb NPs-SCFs and Sb MPs/SCFs anodes before cycling; (d-f) Electrode thickness of Sb NSs-SCFs, Sb NPs-SCFs and Sb MPs/SCFs anodes after 100 cycles

Table S1. Comparisons of selected performance metrics of Sb-based SIBs anodes.

Anode materials	Current density (mAg^{-1})	Cycle number	Reversible capacity ($mAh\ g^{-1}$)	Refs.
α-Sb/NC	100	100	479.6	[S1]
Sb-300	0.5 C	100	531	[S2]
Peapod-like Sb@C	1000	3000	305	[S3]
Sb@(N, S-C)	100	150	621.1	[S4]
Sb_2S_3/SGS	2000	900	524.4	[S5]
Sb@Void@GDY NB	100	200	593	[S6]
Sb/C	100	200	380	[S7]
Sb/N-CNN	1000	6000	401	[S8]
Sb_2O_3@Sb@NC	10000	10000	245.2	[S9]
Sb@P-N/C	50	200	500.1	[S10]
Sb NPs-SCFs	1000	200	381.9	This work

References

S1 J. Yang, J. Li, T. Wang, P. H. L. Notten, H. Ma, Z. Liu, C. Wang and G. Wang, *Chem. Eng. J.*, 2021, **407**, 127169.

S2 X. Li, M. Sun, J. Ni and L. Li, *Adv. Energy Mater.*, 2019, **9**, 1901096.

S3 K. Yang, J. Tang, Y. Liu, M. Kong, B. Zhou, Y. Shang and W.-H. Zhang, *ACS Nano*, 2020, **14**, 5728–5737.

S4 C. Cui, J. Xu, Y. Zhang, Z. Wei, M. Mao, X. Lian, S. Wang, C. Yang, X. Fan, J. Ma and C. Wang, *Nano Lett.*, 2019, **19**, 538–544.

S5 X. Xiong, G. Wang, Y. Lin, Y. Wang, X. Ou, F. Zheng, C. Yang, J.-H. Wang and M. Liu, *ACS Nano*, 2016, **10**, 10953–10959.

S6 Y. Liu, Y. Qing, B. Zhou, L. Wang, B. Pu, X. Zhou, Y. Wang, M. Zhang, J. Bai, Q. Tang and W. Yang, *ACS Nano*, 2023, **17**, 2431–2439.

S7 Z. Liu, X.-Y. Yu, X. W. (David) Lou and U. Paik, *Energy Environ. Sci.*, 2016, **9**, 2314–2318.

S8 W. T. Jing, Y. Zhang, Y. Gu, Y. F. Zhu, C. C. Yang and Q. Jiang, *Matter*, 2019, **1**, 720–733.

S9 A. Xu, C. Huang, G. Li, K. Zou, H. Sun, L. Fu, J. Ju, Y. Song, S. Wu, Z. Xu and Y. Yan, *J. Mater. Chem. A*, 2021, **9**, 12169–12178.

S10 N. Zhang, X. Chen, J. Xu, P. He and X. Ding, *ACS Appl. Mater. Interfaces*, 2023, **15**, 26728–26736.

Table S2. Impedance parameters of Sb NSs-SCFs, Sb NPs-SCFs and Sb MPs/SCFs anodes before and after 100 cycles at 0.1 A g^{-1}

	Components	Rs (Ω)	Rct (Ω)
Before cycling	Sb NSs-SCFs	3.34	227.4
	Sb NPs-SCFs	6.1	221
	Sb MPs/SCFs	3.09	309
After 100 cycles	Sb NSs-SCFs	1.6	179.6
	Sb NPs-SCFs	1.07	137.7
	Sb MPs/SCFs	14.7	569.4